



Genotype–phenotype correlation in patients with Usher syndrome and pathogenic variants in *MYO7A*: implications for future clinical trials

Lilián Galbis-Martínez,^{1,2,†} Fiona Blanco-Kelly,^{1,2,†} Gema García-García,^{2,3,4,†} Almudena Ávila-Fernández,^{1,2} Teresa Jaijo,^{2,3,4} Carla Fuster-García,^{2,3,4} Irene Perea-Romero,^{1,2} Olga Zurita-Muñoz,^{1,2} Belén Jimenez-Rolando,^{2,5} Ester Carreño,^{2,5} Blanca García-Sandoval,^{2,5} José M. Millán^{2,3,4,§}  and Carmen Ayuso^{1,2,§} 

¹Department of Genetics, University Hospital Fundacion Jimenez Diaz, IIS-FJD, UAM, Madrid, Spain

²CIBERER, ISCIII, Madrid, Spain

³Unit of Genetics, University Hospital La Fe – IIS La Fe, Valencia, Spain

⁴Joint Unit for Rare Diseases IIS La Fe-CIPF, Valencia, Spain

⁵Department of Ophthalmology, University Hospital Fundacion Jimenez Diaz, IIS-FJD, UAM, Madrid, Spain

ABSTRACT.

Purpose: We aimed to establish correlations between the clinical features of a cohort of Usher syndrome (USH) patients with pathogenic variants in *MYO7A*, type of pathogenic variant, and location on the protein domain.

Methods: Sixty-two USH patients from 46 families with biallelic variants in *MYO7A* were examined for visual and audiological features. Participants were evaluated based on self-reported ophthalmological history and ophthalmological investigations (computerized visual field testing, best-corrected visual acuity, and ophthalmoscopic and electrophysiological examination). Optical coherence tomography and fundus autofluorescence imaging were performed when possible. Auditory and vestibular functions were evaluated. Patients were classified according to the type of variant and the protein domain where the variants were located.

Results: Most patients displayed a typical USH1 phenotype, that is, prelingual severe-profound sensorineural hearing loss, prepubertal retinitis pigmentosa (RP) and vestibular dysfunction. No statistically significant differences were observed for the variables analysed except for the onset of hearing loss due to the existence of two USH2 cases, defined as postlingual sensorineural hearing loss, postpubertal onset of RP, and absence of vestibular dysfunction, and one atypical case of USH.

Conclusion: We were unable to find a correlation between genotype and phenotype for *MYO7A*. However, our findings could prove useful for the assessment of efficacy in clinical trials, since the type of *MYO7A* variant does not seem to change the onset, severity or course of visual disease.

Key words: clinical trials – genetic screening – *MYO7A* – genotype–phenotype correlation – Usher syndrome

[†]These authors contributed equally.

[§]These authors contributed equally.

Introduction

Usher syndrome (USH) is an autosomal recessive and genetically heterogeneous disorder characterized by bilateral sensorineural hearing loss, retinitis pigmentosa (RP), and, sometimes, vestibular dysfunction (Millán et al. 2011). It is the main cause of blindness in combination with deafness (Vernon 1969), and its prevalence ranges from 3.2 to 6.2 per 100,000 people, depending on the population (Boughman et al. 1983; Hope 1997; Espinós et al. 1998).

The three clinical types of USH are USH type 1 (USH1, MIM#276900), USH type 2 (USH2, MIM#276901) and USH type 3 (USH3, MIM#276903), which are distinguishable by their hearing and vestibular phenotypes (Saihan et al. 2009; Millán et al. 2011). USH2 is characterized by stable, moderate-to-severe hearing loss and normal vestibular function. The USH3 phenotype is characterized by progressive loss of hearing and variable degrees of vestibular dysfunction (Kimberling & Moller 1995). Of the three clinical groups, USH1 is the most disabling, since it is characterized by profound congenital hearing loss, absence of vestibular function, and earlier onset of RP than in USH2 and USH3 (Blanco-Kelly et al. 2015). Children with USH1 have delayed

Acta Ophthalmol. 2021; 99: 922–930

© 2021 The Authors. Acta Ophthalmologica published by John Wiley & Sons Ltd on behalf of Acta Ophthalmologica Scandinavica Foundation

This is an open access article under the terms of the Creative Commons Attribution-NonCommercial-NoDerivs License, which permits use and distribution in any medium, provided the original work is properly cited, the use is non-commercial and no modifications or adaptations are made.

doi: 10.1111/aos.14795

motor development secondary to abnormal vestibular and hearing function. Speech acquisition may be further affected if deafness is not corrected early (Petit 2001). While cochlear implantation has proven to be an effective approach to correct hearing loss (Jatana et al. 2013), there is currently no cure for RP in USH patients.

The six genes involved in USH1 are *MYO7A* (MIM #276903), *USH1C* (MIM #605242), *CDH23* (MIM #605516), *PCDH15* (MIM #605514), *USH1G* (MIM #607696) and *CIB2* (MIM #605564). *MYO7A*, is the most frequently mutated in USH1, accounting for 29–50% of all cases (Weil et al. 1995; Bharadwaj et al. 2000; Ouyang et al. 2005; Jaijo et al. 2006; Roux et al. 2006; Oshima et al. 2008; Le Quesne Stabej et al. 2012; Bonnet et al. 2016). Mutations in *MYO7A* cause not only USH1, but also dominant or recessive isolated sensorineural hearing loss (Tamagawa et al. 2002; Riazuddin et al. 2008).

MYO7A encodes myosin VIIa, an actin-based motor protein comprising several functional domains, as follows: (1) the N-terminal motor (or head)

domain, which contains the actin-binding site and the ATP-binding site; (2) the neck region, with five IQ that bind calmodulin; and (3) the tail region, including two large tandem repeats separated by an SH3 (src homology-3) motif and containing the MyTH4 (myosin tail homology 4) and FERM (4.1 ezrin, readixin, moesin) domains. FERM mediates attachment to the plasma membrane through its interaction with harmonin (Reiners et al. 2006; Yu et al. 2017) (Fig. 1).

Myosin VIIa is expressed in the inner ear and in the retina. In the ear, it is essential for the development of the hair bundle of the cochlea and vestibular system, and for mechano-electrical transduction in the hair cells (Self et al. 1998; Boëda et al. 2002; Kros et al. 2002). In the retina, it is expressed in rod and cone photoreceptor cells and in the retinal pigment epithelium, where it plays an important role in photoreceptor opsin transport through the connecting cilium and in the movement of melanosomes and phagosomes (Liu et al. 1998; Liu et al. 1999; Gibbs et al. 2004).

Here, we retrospectively describe the phenotype of a cohort of 62 USH patients genetically diagnosed with mutations in *MYO7A* in order to outline a retrospective cross-sectional study of the disease and to detect correlations with genotype.

Methods

Patients

The study population comprised 62 patients from 46 families with a clinical diagnosis of USH1 or USH2 and carrying biallelic causative variants in *MYO7A*. The patients were referred from the Federación de Asociaciones de Distrofias de Retina de España (FARPE) and from several Spanish hospitals and were recruited at the Genetics Department of the Fundación Jiménez Díaz Hospital (Madrid, Spain). Molecular analyses were performed by the Genetics Department of University Hospital La Fe (Valencia, Spain) or by the Clinical Genetics Department of Fundación Jiménez Díaz Hospital (Madrid, Spain).

Whenever possible (29 families), samples from family members were

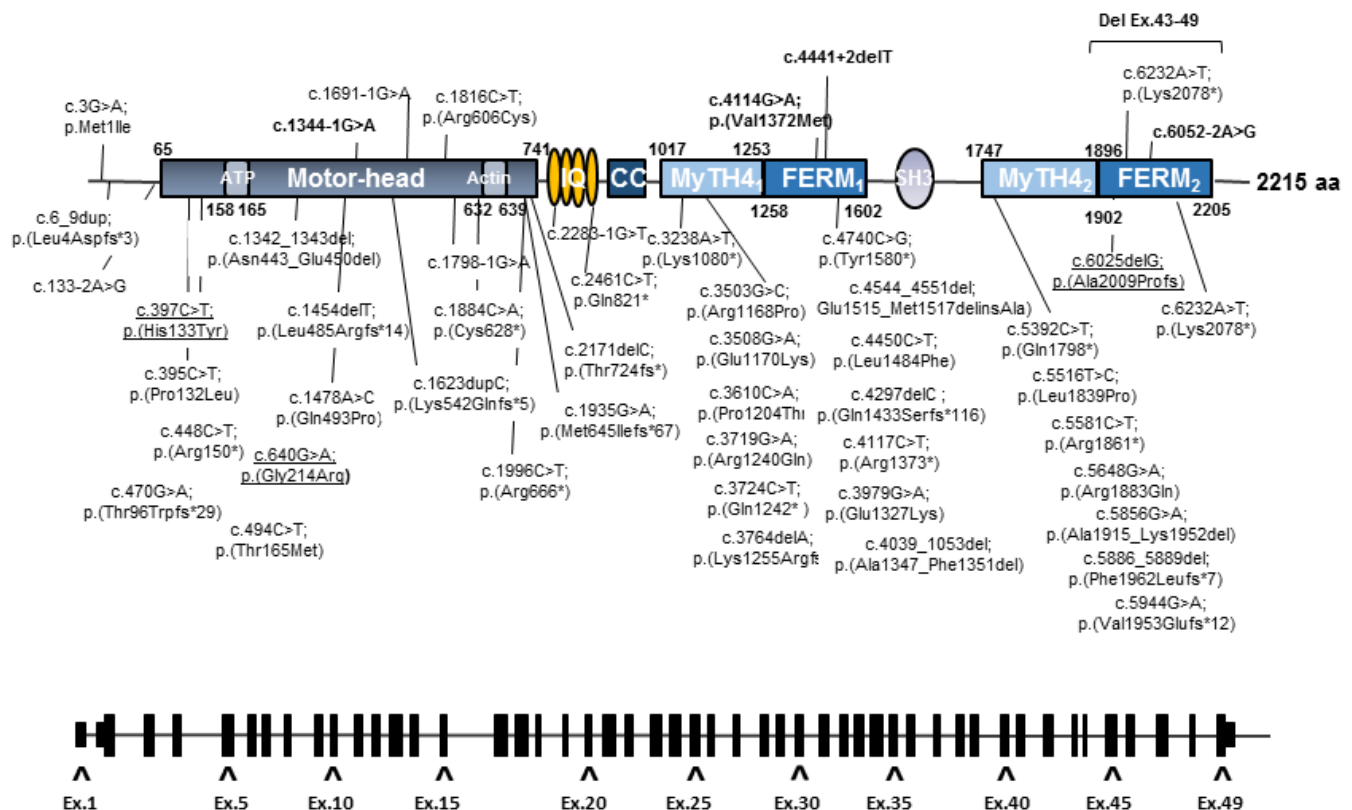


Fig. 1. MYO7A protein structure showing its functional domains.

used for segregation analysis of the variants identified in the index patient. Family pedigrees of segregated families are shown in Fig. S1.

Written informed consent was obtained from all patients and their relatives. All investigations were reviewed and approved by the Ethics Committee of the hospital and conducted in accordance with the principles of the Declaration of Helsinki and its revisions.

Clinical evaluation

Usher syndrome was diagnosed on the basis of simultaneous occurrence of sensorineural deafness and retinal dystrophy. Phenotypic classification into USH clinical types was performed as described previously (Smith et al. 1994).

Fifty-four patients (39 families) and 55 cases (40 families) were evaluated to determine their ophthalmological and audiological phenotype, respectively.

The ophthalmological evaluation consisted of a self-reported ophthalmological history recorded from questionnaires (including onset of symptoms, age at diagnosis, and family history), and objective ophthalmological studies, which included computerized central and peripheral visual field testing, best-corrected visual acuity, ophthalmoscopic examination after pupillary dilation, and electrophysiological examination (full-field electroretinogram). In some cases, optical coherence tomography (OCT) and fundus autofluorescence (FAF) imaging were recorded.

Auditory and vestibular functions were assessed by complete examination whenever possible. Patients with no islands of hearing and no response better than 90 dB along the standard test frequencies were classified as USH1.

Genetic analysis

Peripheral blood samples of index cases and family members were collected in EDTA tubes. DNA was extracted as described elsewhere (Blanco-Kelly et al. 2015).

Several approaches were used for molecular characterization, since USH patients were genetically diagnosed during a period when various molecular techniques were developed and

implemented in the laboratory, as follows: (1) sequencing of all exons and flanking intronic regions of *MYO7A*; (2) a specific USH genotyping microarray (AsperBiotech, Tartu, Estonia); (3) comparative genomic hybridization microarray (CGH-microarray) chip including the USH genes for detecting large genomic rearrangements; (4) targeted next-generation sequencing (NGS); (5) Clinical exome: TruSight-One (Illumina) or Clinical Exome Solution (Sophia Genetics, Saint Sulpice, Switzerland), using the NextSeq platform (Illumina, Inc, San Diego, CA, USA).

Suspected pathogenic variants and familial segregation studies were confirmed using Sanger sequencing.

In silico analysis of variants

Variants found in *MYO7A* were checked against the following databases: LOVD (https://grenada.lumc.nl/LSDB_list/lsdbs/MYO7A), Human Gene Mutation Database (<http://www.hgmd.cf.ac.uk/> Professional 2018.2) and ClinVar (<https://www.ncbi.nlm.nih.gov/clinvar/>). The pathogenicity of novel missense variants was analysed using four predictive software programs: (1) SIFT (<http://sift.bii.a-star.edu.sg/>), (2) Polyphen-2 (<http://genetics.bwh.harvard.edu/pph2/>), (3) M-CAP (<http://bejerano.stanford.edu/mcap/>) and (4) Mutation Taster. Putative variants affecting the splicing process were studied using NNSPLICE v0.9 (http://www.fruitfly.org/seq_tools/splice.html), Human Splicing Finder (HSF; Human Splicing Finder), Splice Site Finder, MaxEntScan and Gene Splicer. Each software application uses an algorithm that gives a range of values. For instance, consensus values go from 0 to 100 for Human Splicing Finder, -20 to +20 for MaxEntScan, and 0 to 1 for NNSplice. The threshold is defined at 65 for HSF, 3 for MaxEnt, and according to the operator for NNSplice. Therefore, every signal with a score above the threshold is considered to be a splice site (donor or acceptor). A value below the threshold is predicted to abolish the splice site.

Novel rare variants were checked against the Genome Aggregation Database (gnomAD Exomes and gnomAD Genomes), 1000 Genomes Project, Exome Variant Server (EVS), Exome

Aggregation Consortium (ExAC), and Collaborative Spanish Variant Server (created by CIBERER-BIER: <http://csvs.babelomics.org>).

The nomenclature of *MYO7A* variants was drafted according to the reference sequence NM_000260.3.

Statistical analysis

Patients were grouped based on mutation type and mutation protein location.

Group 1: According to genotype mutation, as follows: category A, missense/missense; B, missense/truncating; and C, truncating/truncating.

Group 2: According to the protein domain where the mutation was located, as follows: category 1, motor/motor; 2, motor/tail₁; 3, tail₁/tail₁; 4, motor/neck; 5, neck/neck; 6, neck-tail₁; 7, motor/-tail₂; 8, tail₂/tail₂; and 9, tail₁/tail₂ ('motor', motor-head domain; 'neck', region linking the motor-head and tail regions; 'tail₁', region comprising the MyTH4₁-FERM₁ domains; and 'tail₂', fragment containing the MyTH4₂-FERM₂ domains).

The survival curves for years free of visual acuity (VA) under 0.1 (decimal), years free of visual field lower than 10°, and years free of cataracts were estimated using the Kaplan–Meier method. These analyses were based on available clinical data obtained from ophthalmological examinations (not self-reported). Curves were compared by means of the log-rank test.

The variables age at diagnosis, onset of night blindness, onset of visual field constriction, onset of visual acuity reduction, onset of hearing loss and age of onset (months) at unaided walking (based on self-reported data) were compared for all categories according to group 1 and group 2 using the Kruskal–Wallis test.

Haplotype analysis

To determine whether the most prevalent mutations in our cohort shared haplotypes among affected families, we selected the following for haplotype analysis: three single intragenic nucleotide polymorphisms (SNPs), namely, rs6592706, rs948972 and rs11237122 (Roberts et al. 2015), and three polymorphic markers spanning the USHB1 locus, namely, D11S787,

D11S527 and D11S4186 (Adato et al. 1997). The primers used are listed in Table S1.

The location of each marker referring to the *MYO7A* gene and to the most prevalent *MYO7A* variants found in this study is depicted in Fig. S2.

Results

Clinical features

Clinical information was limited for some patients, since they were referred to our hospital from other regions of Spain. Electroretinography data were available for 46 patients, of whom 34 (74%) had a nonrecordable ERG and 12 (26%) had recordings with abnormal values. Optical coherence tomography (OCT) was carried out in 51 patients (82%). Only five (8%) patients had cystoid macular oedema.

Most patients displayed a typical USH1 phenotype; three were classified as atypical USH or USH2 (Table S2). One patient from the RP-1218 family was diagnosed with atypical USH based on the auditory phenotype, since he referred progressive hearing loss beginning at 15 years and his audiometry at 23 years showed a down-sloping pattern, with mild-moderate hypoacusis at low-middle frequencies and moderate-severe hypoacusis at high frequencies (Fig. S3). Patients FRP-159 and RP-2947 were classified as USH2. The FRP-159 patient presented with moderate hearing loss and intelligible speech, and patient RP-2947 had

more severe hypoacusis, although this was diagnosed later (at 3 years) and corrected with hearing aids at the age of 9 years. This patient had a more attenuated ophthalmological phenotype, with no symptoms of loss of visual acuity at the age of 65 years.

When available, OCT disclosed the expected loss of outer retina concentrically in the periphery of the macular area, with total disorganization of the ellipsoid layer and outer retina in the most severe cases. Some patients had macular oedema with intraretinal fluid in areas overlying a preserved ellipsoid layer. Blue-peak FAF—when available—revealed peripheral loss of FAF with a hyperautofluorescent concentric halo in all patients.

The overall mean age at diagnosis for patients with mutations in *MYO7A* was 14.86 ± 10.37 years. Age of onset by condition was as follows: night blindness, 13.23 ± 9.47 years; onset of reduced visual field, 13.87 ± 8.91 years; loss of visual acuity, 19.88 ± 11.83 years; diagnosis of hearing loss, 11.83 ± 9.1 months; and unaided walking, 22.89 ± 10.88 months.

Molecular characterization

Forty-nine distinct pathogenic/likely pathogenic variants were identified in the 46 families. Patients from 22 of these families were homozygous, and 24 were compound heterozygous. Consanguinity was observed in 10 of the 22 homozygous families. Changes

included missense, frameshift, nonsense, small and gross deletions and variants likely affecting splicing, the most frequent being those leading to a truncated protein (57 out of 92 alleles). The mutations observed in the present report are detailed in Table S3.

Patients were distributed as follows:
Grouping 1: type of mutation

1 Categories (cases):

- a A: missense/missense (15)
- b B: missense/truncating (15)
- c C: truncating/truncating (32)

Grouping 2: protein domain affected by the mutation

1 Categories (cases):

- a 1: motor/motor (22)
- b 2: motor/tail₁ (4)
- c 3: tail₁/tail₁ (8)
- d 4: motor/neck (2)
- e 5: neck-neck (4)
- f 6: neck-tail₁ (3)
- g 7: motor-tail₂ (5)
- h 8: tail₂/tail₂ (8)
- i 9: tail₁/tail₂ (6)

The positions of the variants observed along the myosin VIIA structural domains are depicted in Fig. 1.

Only three of the detected mutations were located upstream of the motor domain, and two were located at the IQ motif. These last five changes were severe mutations that may prevent the correct start or produce a premature termination of the protein translation or create an aberrant transcript.

Table 1. Pathogenic predictions of novel (exonic and intronic) variants by several computational programs. 'X → Y' indicates the reduction in the score for the main donor or acceptor site from 'X' to 'Y'.

<i>MYO7A</i> variant	Protein		SIFT (score)		PolyPhen-2 (score)		MutationTaster	M-CAP (score)
c.4114G>A delE43-E49	p.(Val1372Met) c.5857-?_*544+?del		Deleterious (0.02)		Prob. damaging (0.999)		Disease-causing	Possibly pathogenic (0.086)
<i>MYO7A</i> variant	Intron	Splice Site Finder	MaxEntScan	NNSPLICE	Gene Splicer	Human Splicing Finder	Predicted consequence	
c.1344-1G>A	12	82 → 0	10 → 0	1 → 0	11 → 0	88 → 0	Possible effect at nearest splice site	
c.4441+2delT	33	71 → 0	9 → 0	1 → 0	3 → 0	99 → 0	Possible effect at nearest splice site	
c.6052-2A>G	44	90 → 0	10 → 0	1 → 0	12 → 0	89 → 0	Possible effect at nearest splice site	

Each software uses an algorithm that provides a range of values. For instance, consensus values run from 0 to 100 for Human Splicing Finder, from -20 to +20 for MaxEntScan, and from 0 to 1 for NNSplice. The threshold is defined at 65 for HSF, 3 for MaxEnt, and according to the operator for NNSplice. Consequently, every signal with a score above the threshold is considered to be a splice site (donor or acceptor). A value below the threshold is predicted to abolish the splice site.

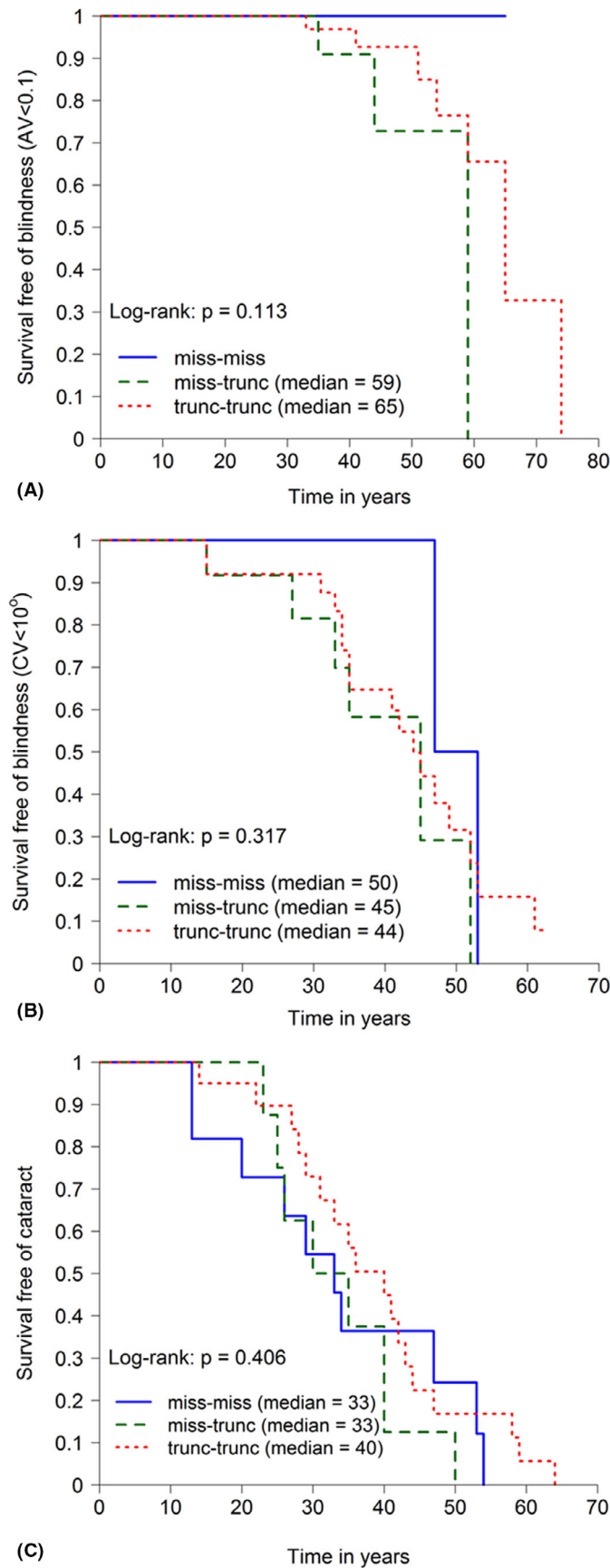


Fig. 2. Survival curves. (A) Blindness-free survival on the basis of visual acuity (blindness VA < 0.1). (B) Blindness-free survival on the basis of visual field (blindness VF < 10°). (C) Blindness-free survival on the basis of age of onset of cataracts.

The most prevalent variants detected were as follows: c.397C>T and p.(His133Tyr), found in three homozygous patients (six alleles); c.640G>A and p.(Gly214Arg), found in four unrelated patients (five alleles); and c.6025delG and p.(Ala2009Profs*32), found in two homozygous and in one heterozygous patient (five alleles). Only 13 of the variants were found in more than one of the families (36 of the variants were found in only one family in our cohort).

Five of the alleles identified in *MYO7A* (10%) had not been previously reported. Screening for potentially causative missense and splice novel variants was performed using prediction software programs. In the case of missense variants, those predicted as damaging by at least two different prediction programs in an evolutionary conserved residue (Table 1), and not found in the general population, and cosegregating with the disease (when DNA of relatives were available) were initially considered potentially pathogenic (Table S4). For splice variants, the software programs applied used algorithms with a threshold for prediction of the effect on the splice site; Table 1 shows how the high scores obtained for the wild-type variants decrease to zero for the mutations c.1344-1G>A, c.4441+2delT and c.6052-2A>G, thus implying that they alter the nearest splice site; therefore, we considered them to be pathogenic.

Statistical analysis

Blindness-free survival in years is shown in Fig. 2. A visual acuity value under 0.1 was reached at a median of 65 years by patients who carried two truncating mutations and at almost 60 years by those who had a combination of one missense mutation and one truncating mutation (Fig. 2A). A visual field lower than 10° was reached at 44 and 45 years for patients with two truncating mutations and a combination of a missense and a truncating mutation, respectively, and at 50 years of age for those bearing two missense mutations (Fig. 2B). Cataracts appeared at a median age of 40 years for patients with two truncating mutations and 33 years for those carrying two missense mutations and those with one missense mutation and one truncating mutation (Fig. 2C).

A tendency towards later onset of symptoms in patients carrying two truncating mutations was observed; however, these differences were not statistically significant. The p values were 0.113, 0.317 and 0.406 for visual acuity, visual field and cataract, respectively.

No statistically significant differences were observed for any visual variable (age at diagnosis, onset of night blindness, reduction of visual field or visual acuity) except for onset of hearing loss (mean 0.7–17.9) due to atypical USH and USH2 (Table 2).

Similarly, no statistically significant differences were found when variables were categorized according to the altered protein domain (Table 3).

Haplotype analysis

In order to explore the possible founder effect of the most frequent *MYO7A* variants in the Spanish population, we performed haplotype studies on the most recurrent *MYO7A* variants found in this study (c.640G>A, c.397C>T and c.6025delG) (Fig. S4). Families carrying the c.640G>A mutation were from the same Spanish region (Castilla-La Mancha), whereas families with c.397C>T or c.6025delG variants came from different, distant Spanish locations. A haplotype was associated with each of the three mutations. In the families in the present study, haplotypes were shared by all the patients who carried the same mutation, thus suggesting a common origin for each of them.

Discussion

More than 500 variants within the gene encoding myosin VIIA have been described to date, and most are private mutations (HGMD, Human Gene Mutation Database, <https://portal.bioinformatics.org/hgmd/pro/gene.php?gene=MYO7A>). We screened for mutations in 46 families with USH, mainly type I, and detected 49 different

Table 2. Mean and standard deviation, median (in years, except for onset of hearing loss and unaided walking [in months]) and p value of the age of onset for the analysed features among patients categorized on the basis of the mutation type.

Variable	Group	n	Mean ± SD	Median (IQR)	p value
Age at diagnosis	miss-miss	13	11.9 ± 5.9	11.0 (6.0)	0.268
	miss-trunc	11	18.8 ± 10.1	13.0 (14.0)	
	trunc-trunc	23	15.1 ± 11.2	12.0 (7.5)	
Onset of night blindness	miss-miss	7	8.6 ± 3.9	8.0 (4.5)	0.298
	miss-trunc	8	12.6 ± 4.8	10.5 (5.0)	
	trunc-trunc	22	14.0 ± 11.0	11.5 (6.8)	
Onset of visual field constriction	miss-miss	7	9.9 ± 5.7	10.0 (9.0)	0.333
	miss-trunc	9	17.3 ± 10.6	14.0 (9.0)	
	trunc-trunc	24	13.5 ± 8.7	12.0 (4.8)	
Onset of visual acuity reduction	miss-miss	7	17.4 ± 10.8	14.0 (13.0)	0.738
	miss-trunc	9	21.1 ± 11.6	20.0 (20.0)	
	trunc-trunc	17	22.0 ± 14.5	18.0 (22.0)	
Onset of hearing loss (months)	miss-miss	13	3.0 ± 5.7	0.0 (3.0)	0.008
	miss-trunc	12	17.9 ± 51.2	1.5 (8.0)	
	trunc-trunc	25	0.7 ± 3.6	0.0 (0.0)	
Unaided walking (months)	miss-miss	3	27.7 ± 9.7	30.0 (9.5)	0.220
	miss-trunc	6	17.8 ± 1.5	18.5 (2.5)	
	trunc-trunc	8	25.4 ± 11.0	21.5 (9.0)	

miss-miss = missense-missense genotype, miss-trunc = missense-truncating genotype, IQR = interquartile range, SD = standard deviation, trunc-trunc = truncating-truncating genotype.

Table 3. Mean and standard deviation, median (in years, except for hearing loss and unaided walking [in months]) and p value of the onset for the features analysed categorized on the basis of the protein domain that is affected by the mutations (only missense mutations).

Variable	Group	n	Mean ± SD (years)	Median (IQR) (years)	p value
Age at diagnosis	motor-motor	14	12.8 ± 7.7	11.0 (5.8)	0.277
	motor-tail ₁	4	18.0 ± 9.6	19 (11.5)	
	tail ₁ -tail ₁	7	10.0 ± 6.1	10.0 (2.5)	
	motor-neck	2	11.0 ± 1.4	11.0 (1.0)	
	neck-neck	2	12.0 ± 0.0	12.0 (0.0)	
	neck-tail ₁	2	14.0 ± 1.4	14.0 (1.0)	
	motor-tail ₂	4	22.0 ± 7.4	25.0 (4.0)	
	tail ₂ -tail ₂	6	17.0 ± 12.3	13.0 (7.3)	
	tail ₁ -tail ₂	5	9.8 ± 3.4	11.0 (1.0)	
Onset of night blindness	motor-motor	12	9.5 ± 9.0	7.5 (5.5)	0.068
	motor-tail ₁	3	12.0 ± 2.0	12.0 (2.0)	
	tail ₁ -tail ₁	7	16.0 ± 11.6	12.0 (3.5)	
	motor-neck	2	9.0 ± 1.4	9.0 (1.0)	
	neck-neck	2	28.5 ± 14.8	28.5 (10.5)	
	neck-tail ₁	2	14.0 ± 1.4	14.0 (1.0)	
	motor-tail ₂	4	14.5 ± 6.4	15 (10.5)	
	tail ₂ -tail ₂	3	8.3 ± 3.1	9.0 (3.0)	
	tail ₁ -tail ₂	3	10.3 ± 3.8	12.0 (3.5)	
Onset of visual field constriction	motor-motor	12	12.0 ± 9.1	11.5 (9.5)	0.242
	motor-tail ₁	3	8.3 ± 4.9	6.0 (4.5)	
	tail ₁ -tail ₁	7	11.6 ± 2.6	11.0 (3.5)	
	motor-neck	2	9.3 ± 1.8	9.3 (1.3)	
	neck-neck	2	15.0 ± 4.2	15.0 (3.0)	
	neck-tail ₁	2	14.0 ± 1.4	14.0 (1.0)	
	motor-tail ₂	4	20.3 ± 7.8	20 (4.8)	
	tail ₂ -tail ₂	5	18.0 ± 13.6	14.0 (7.0)	
	tail ₁ -tail ₂	3	8.7 ± 4.2	10.0 (4.0)	
Onset of visual acuity reduction	motor-motor	12	23.7 ± 16.6	18.5 (23.0)	0.238
	motor-tail ₁	2	31.5 ± 2.1	31.5 (1.5)	
	tail ₁ -tail ₁	4	9.5 ± 4.2	10.0 (4.0)	
	neck-neck	2	26.5 ± 12	26.5 (8.5)	
	neck-tail ₁	2	14.0 ± 1.4	14.0 (1.0)	
	motor-tail ₂	4	17.8 ± 10.7	18.5 (8.8)	
	tail ₂ -tail ₂	6	14.5 ± 8.3	14.0 (13.3)	
	tail ₁ -tail ₂	1	35.0 ± NC	35.0 (0.0)	
Onset of hearing los (months)	motor-motor	16	2.3 ± 5.2	0.0 (0.0)	0.296
	motor-tail ₁	4	5.3 ± 8.6	1.5 (6.8)	
	tail ₁ -tail ₁	8	3.3 ± 3.8	1.5 (7.3)	
	motor-neck	2	0.0 ± 0.0	0.0 (0.0)	
	neck-neck	2	0.0 ± 0.0	0.0 (0.0)	
	neck-tail ₁	3	0.0 ± 0.0	0.0 (0.0)	
	motor-tail ₂	4	47 ± 88.7	4.0 (51.0)	
	tail ₂ -tail ₂	6	0.0 ± 0.0	0.0 (0.0)	
	tail ₁ -tail ₂	5	0.6 ± 1.3	0.0 (0.0)	
Start walking (months)	motor-motor	5	24.2 ± 8.6	22.0 (13.0)	0.324
	tail ₁ -tail ₁	4	20.0 ± 2.7	19.0 (1.5)	
	motor-neck	1	36.0 ± NC	36.0 (0.0)	
	neck-neck	1	18.0 ± NC	18.0 (0.0)	
	neck-tail ₁	1	48.0 ± NC	48.0 (0.0)	
	motor-tail ₂	1	18.0 ± NC	18.0 (0.0)	
	tail ₁ -tail ₂	4	17.8 ± 2.4	17.0 (2.8)	

IQR = interquartile range, SD = standard deviation.

mutations. Of these, five were novel, with absence of hot spot mutations. The results illustrate the high diversity of mutations responsible for USH1B and the absence of a predominant mutation, at least in the Spanish population.

The three recurrent mutations (c.640G>A, c.397C>T and c.6025delG)

in our study have also been identified worldwide in different populations (<https://databases.lovd.nl/shared/genes/MYO7A>). We found that each was associated with a common haplotype, suggesting a common ancestral origin, at least in Spain.

Our phenotyping results for *MYO7A* patients are very similar to

those reported by Blanco-Kelly (Blanco-Kelly et al. 2015) in a study carried out in the Spanish population including USH1 patients with mutations in *MYO7A*, *CDH23*, *PCDH15*, *USH1C* and *SANS*, in which the mean age at onset of hearing loss was 1.1 ± 0.5 years and the onset of visual symptoms was 9.5 ± 8 years (Blanco-

Kelly et al. 2015). This is not striking, since more than 50% of cases of USH1 in our study were due to *MYO7A* mutations.

In genes such as the *USH2A* gene, missense mutations lead to a less severe phenotype than truncating mutations (Pérez-Carro et al. 2018). While this might have been expected for *MYO7A*, our results indicate that there is no straightforward correlation between the severity of the USH1 phenotype and the type of mutation in *MYO7A* (Rong et al. 2014).

No statistically significant differences were recorded for the variables analysed, although this could be because of insufficient statistical power. As can be observed, there is a slight difference for carriers of two missense mutations, in whom onset of visual symptoms seems to be earlier than in those with two truncating mutations. The lack of genotype–phenotype correlation, however, could also be due to the absence of genotype–phenotype for *MYO7A*.

The only significant variable (*p* value: 0.007) was age at onset of hearing loss. It is well known that USH1 is defined by congenital or very early profound sensorineural hearing loss. In our series, hearing loss was detected within the first year of life in most cases. But the differences observed in the present series are due to three cases diagnosed of either atypical USH or USH2, mainly patient RP-1218.

Another bias to be borne in mind is that this study was based to a certain degree on patient recall for some variables, and this might reduce the likelihood of detecting any real difference, especially if the difference is small.

Patients with an atypical phenotype associated with *MYO7A* are not infrequent, and mutations in *MYO7A* have been associated with diverse clinical phenotypes. A number of studies have reported patients with mutations in *MYO7A* who are clinically USH2 (Bonnet et al. 2011, 2016; Rong et al. 2014).

Despite the efforts of many researchers to establish a genotype–phenotype correlation for inherited retinal dystrophies, this correlation has proven elusive for most of the genes involved (Sorrentino et al. 2016).

For the last few years, next-generation sequencing has made it possible to

screen large series of patients and a large number of genes, thus enabling a correlation with phenotype to be established for mutations in some genes (eg, *ABCA4*, *RHO*, *EYS* and *CRB1*) (Boulangier-Scemama et al. 2015; Fernandez-San Jose et al. 2015; Nassisi et al. 2018).

A similar phenotype–genotype correlation has been defined for the p.(Cys579Phe) variant, for which, depending on its zygosity in the *USH2A* gene, distinguishable phenotypes can be identified (Pérez-Carro et al. 2018).

In contrast, a genotype–phenotype correlation seems to be difficult to establish for other genes, such as *MYO7A*. Thus, the current study could be useful for further assessment of efficacy in clinical trials, as it provides a detailed phenotype description for *MYO7A* and suggests that the onset, severity and progression of visual disease is not determined by the type of mutation in *MYO7A* or its location.

In most cases, mutations in *MYO7A* lead to USH1. However, the phenotypic range of *MYO7A* is wide, leading to USH2 and nonsyndromic hearing loss. The study of *MYO7A* must be borne in mind in USH2 patients who do not harbour mutations in the USH2 genes, since they may benefit from current and forthcoming retinal therapeutic strategies based on gene therapy.

In the era of gene-based therapeutic strategies, our study could be useful for the assessment of efficacy in clinical trials. Furthermore, our data will improve counselling of patients and relatives on the clinical onset and prognosis of the disease.

References

Adato A, Weil D, Kalinski H, Pel-Or Y, Ayadi H, Petit C, Korostishevsky M & Bonne-Tamir B (1997): Mutation profile of all 49 exons of the human myosin VIIA gene, and haplotype analysis, in Usher 1B families from diverse origins. *Am J Hum Genet* **61**: 813–821.

Bharadwaj AK, Kasztejna JP, Huq S, Berson EL & Dryja TP (2000): Evaluation of the myosin VIIA gene and visual function in patients with Usher syndrome type I. *Exp Eye Res* **71**: 173–181.

Blanco-Kelly F, Jaijo T, Aller E et al. (2015): Clinical aspects of usher syndrome and the USH2A gene in a cohort of 433 patients. *JAMA Ophthalmol* **133**: 157–164.

Boëda B, El-Amraoui A, Bahloul A et al. (2002): Myosin VIIa, harmonin and cadherin 23, three Usher I gene products that cooperate to shape the sensory hair cell bundle. *EMBO J* **21**: 6689–6699.

Bonnet C, Grati M, Marlin S et al. (2011): Complete exon sequencing of all known Usher syndrome genes greatly improves molecular diagnosis. *Orphanet J Rare Dis* **6**: 21.

Bonnet C, Riahi Z, Chantot-Bastaraud S et al. (2016): An innovative strategy for the molecular diagnosis of Usher syndrome identifies causal biallelic mutations in 93% of European patients. *Eur J Hum Genet* **24**: 1730–1738.

Boughman JA, Vernon M & Shaver KA (1983): Usher syndrome: definition and estimate of prevalence from two high-risk populations. *J Chronic Dis* **36**: 595–603.

Boulangier-Scemama E, El Shamieh S, Démon-tant V et al. (2015): Next-generation sequencing applied to a large French cone and cone-rod dystrophy cohort: Mutation spectrum and new genotype-phenotype correlation. *Orphanet J Rare Dis* **10**: 85.

Espinós C, Millán JM, Beneyto M & Nájera C (1998): Epidemiology of Usher syndrome in Valencia and Spain. *Community Genet* **1**: 223–228.

Fernandez-San Jose P, Blanco-Kelly F, Corton M et al. (2015): Prevalence of Rhodopsin mutations in autosomal dominant Retinitis Pigmentosa in Spain: clinical and analytical review in 200 families. *Acta Ophthalmol* **93**: e38–e44.

Gibbs D, Azarian SM, Lillo C, Kitamoto J, Klomp AE, Steel KP, Libby RT & Williams DS (2004): Role of myosin VIIa and Rab27a in the motility and localization of RPE melanosomes. *J Cell Sci* **117**: 6473–6483.

Hope CI (1997): Usher syndrome in the city of Birmingham – prevalence and clinical classification. *Br J Ophthalmol* **81**: 46–53.

Jaijo T, Aller E, Oltra S et al. (2006): Mutation profile of the *MYO7A* gene in Spanish patients with Usher syndrome type I. *Hum Mutat* **27**: 290–291.

Jatana KR, Thomas D, Weber L, Mets MB, Silverman JB & Young NM (2013): Usher syndrome: characteristics and outcomes of pediatric cochlear implant recipients. *Otol Neurotol* **34**: 484–489.

Kimberling WJ & Moller C (1995): Clinical and molecular genetics of Usher syndrome. *J Am Acad Audiol* **6**: 63–72.

Kros CJ, Marcotti W, Van Netten SM, Self TJ, Libby RT, Brown SDM, Richardson GP & Steel KP (2002): Reduced climbing and increased slipping adaptation in cochlear hair cells of mice with *Myo7a* mutations. *Nat Neurosci* **5**: 41–47.

Le Quesne Stabej P, Saihan Z, Rangesh N et al. (2012): Comprehensive sequence analysis of nine Usher syndrome genes in the UK National Collaborative Usher Study. *J Med Genet* **49**: 27–36.

Liu X, Ondek B & Williams DS (1998): Mutant myosin VIIa causes defective

- melanosome distribution in the RPE of shaker-1 mice. *Nat Genet* **19**: 117–118.
- Liu X, Udovichenko IP, Brown SD, Self TJ, Libby RT, Steel KP & Williams DS (1999): Myosin VIIa participates in opsin transport through the photoreceptor cilium. *J Neurosci* **19**: 6267–6274.
- Millán JM, Aller E, Jaijo T, Blanco-Kelly F, Gimenez-Pardo A & Ayuso A (2011): An update on the genetics of Usher syndrome. *J Ophthalmol* **2011**: 1–8.
- Nassisi M, Mohand-Saïd S, Dhaenens CM et al. (2018): Expanding the mutation spectrum in ABCA4: sixty novel disease causing variants and their associated phenotype in a large French stargardt cohort. *Int J Mol Sci* **19**: E2196.
- Oshima A, Jaijo T, Aller E, Millán JM, Carney C, Usami S, Moller C & Kimberling WJ (2008): Mutation profile of the CDH23 gene in 56 probands with Usher syndrome type I. *Hum Mutat* **29**: 1–11.
- Ouyang XM, Yan D, Du LL et al. (2005): Characterization of Usher syndrome type I gene mutations in an Usher syndrome patient population. *Hum Genet* **116**: 292–299.
- Pérez-Carro R, Blanco-Kelly F, Galbis-Martínez L et al. (2018): Unravelling the pathogenic role and genotype-phenotype correlation of the USH2A p. (Cys759Phe) variant among Spanish families. *PLoS One* **13**: 1–18.
- Petit C (2001): Usher syndrome: from Genetics to Pathogenesis. *Annu Rev Genomics Hum Genet* **2**: 271–297.
- Reiners J, Nagel-Wolfrum K, Jürgens K, Märker T & Wolfrum U (2006): Molecular basis of human Usher syndrome: deciphering the meshes of the Usher protein network provides insights into the pathomechanisms of the Usher disease. *Exp Eye Res* **83**: 97–119.
- Riazuddin S, Nazli S, Ahmed ZM et al. (2008): Mutation spectrum of MYO7A and evaluation of a novel nonsyndromic deafness DFNB2 allele with residual function. *Hum Mutat* **29**: 502–511.
- Roberts L, George S, Greenberg J & Ramesar RS (2015): A founder mutation in MYO7A underlies a significant proportion of usher syndrome in indigenous south africans: Implications for the African diaspora. *Invest Ophthalmol Vis Sci* **56**: 6671–6678.
- Rong W, Chen X, Zhao K et al. (2014): Novel and recurrent MYO7A mutations in Usher syndrome type 1 and type 2. *PLoS One* **9**: e97808.
- Roux AF, Fougère V, Le Guédard S et al. (2006): Survey of the frequency of USH1 gene mutations in a cohort of Usher patients shows the importance of cadherin 23 and protocadherin 15 genes and establishes a detection rate of above 90%. *J Med Genet* **43**: 763–768.
- Saihan Z, Webster AR, Luxon L & Bitner-Glindzicz M (2009): Update on Usher syndrome. *Curr Opin Neurol* **22**: 19–27.
- Self T, Mahony M, Fleming J, Walsh J, Brown SD & Steel KP (1998): Shaker-1 mutations reveal roles for myosin VIIA in both development and function of cochlear hair cells. *Development* **125**: 557–566.
- Smith RJH, Berlin CI, Hejtmancik JF et al. (1994): Clinical diagnosis of the Usher syndromes. Usher syndrome Consortium. *Am J Med Genet* **50**: 32–38.
- Sorrentino FS, Gallenga CE, Bonifazzi C & Perri P (2016): A challenge to the striking genotypic heterogeneity of retinitis pigmentosa: a better understanding of the pathophysiology using the newest genetic strategies. *Eye* **30**: 1542–1548.
- Tamagawa Y, Ishikawa K, Ishikawa K, Ishida T, Kitamura K, Makino S, Tsuru T & Ichimura K (2002): Phenotype of DFNA11: a nonsyndromic hearing loss caused by a myosin VIIA mutation. *Laryngoscope* **112**: 292–297.
- Vernon M (1969): Usher's syndrome: deafness and progressive blindness. *J Chronic Dis* **22**: 133–151.
- Weil D, Blanchard S, Kaplan J et al. (1995): Defective myosin VIIA gene responsible for Usher syndrome type 1B. *Nature* **374**: 60–61.
- Yu IM, Planelles-Herrero VJ, Sourigues Y et al. (2017): Myosin 7 and its adaptors link cadherins to actin. *Nat Commun* **8**: 1–14.

Received on July 13th, 2020.
Accepted on January 22nd, 2021.

Correspondence:
Carmen Ayuso
Department of Medical Genetics
University Hospital Fundación Jiménez Díaz
Avda. Reyes Católicos, 2
28040 Madrid
Spain
Tel: +34 915 504 872
Fax: +34 961 246 620
Email: Cayuso@fjd.es
José M. Millán
Molecular, Cellular and Genomics
Biomedicine
University Hospital La Fe. Tower A, Floor 4
Avda. Fernando Abril Martorell, 106
46026 Valencia
Spain
Tel: +34 961 246 677
Fax: +34 915 504 849
Email: millan_jos@gva.es

This project was financially supported by the Center for Biomedical Network Research on Rare Diseases (CIBERER), FIS (PI16/00425, PI16/00539 and IIS-FJD Biobank PT13/0010/0012). LG-M and IPR were supported by the Río Hortega and predoctoral Programs (CM16/00126 and FI17/00192, respectively) from Institute of

Health Carlos III (ISCIII, Spanish Ministry of the Economy, Industry and Competitiveness), Regional Government of Madrid (CAM, B2017/BMD37), and Regional Government of the Valencian Community (PROMETEU/2018/135), with partial support from the European Regional Development Fund (ERDF). Additional support was received from the Ramon Areces Foundation, the University Chair UAM-IIS-FJD of Genomic Medicine, ONCE Foundation and the Spanish National Organization of the Blind (ONCE). Drafting of this manuscript was possible thanks to the UshTher project (Clinical trial of gene therapy with dual AAV vectors for retinitis pigmentosa in patients with Usher syndrome type 1B), which has received funding from the European Union's Horizon 2020 research and innovation programme under grant agreement No 754848. The authors are grateful to the families that participated in this study and to the colleagues who referred patients to us. We also thank the Genetics and Ophthalmology Departments of Fundación Jimenez Diaz University Hospital (FJD, Madrid) and Asunción Giménez, Cristina Villaverde, and Ignacio Mahillo for their technical assistance.

Supporting Information

Additional Supporting Information may be found in the online version of this article:

- Table S1.** Name and details of the primers for the amplification of the markers used in the haplotype.
- Table S2.** Genotype and phenotype details of the cohort studied.
- Table S3.** Mutations found in the cohort studied in this work.
- Table S4.** Novel mutations found in this study and their possible effect on the protein.
- Figure S1.** Pedigrees of the 29 segregated families.
- Figure S2.** Diagram representing the *MYO7A* gene and surrounding regions and the relative position of the markers selected for haplotyping. Location of the recurrent mutations is shown by an arrow. umbers in brackets indicate chromosomal position in chromosome 11.
- Figure S3.** Audiograms from patient belonging to family RP-1218 family diagnosed with atypical USH.
- Figure S4.** Haplotype analysis of the three most recurrent *MYO7A* mutations found in this study.